Journal of Cleaner Production 190 (2018) 737–751

Contents lists available at ScienceDirect

Journal of Cleaner Production

journal homepage: www.elsevier.com/locate/jclepro

Electrical and thermal characterisation of cement-based mortars containing recycled metallic waste

J. Norambuena-Contreras [a, *], J. Quilodran [a], I. Gonzalez-Torre [a], M. Chavez [b], R. Borinaga-Treviño [c]

[a] LabMAT, Department of Civil and Environmental Engineering, University of Bío-Bío, Concepción, Chile
[b] Department of Civil Engineering, University Andres Bello, Concepción, Chile
[c] Department of Mechanical Engineering, University of the Basque Country, Bilbao, Spain

ARTICLE INFO

Article history:
Received 5 December 2017
Received in revised form
17 April 2018
Accepted 18 April 2018
Available online 27 April 2018

Keywords:
Cement-based mortars
Metallic waste
Ultrasonic time
Electrical resistivity
Thermal conductivity
Self-monitoring

ABSTRACT

The management and disposal of solid waste from industrial sources is a problem around the world. In recent years, several studies have been carried out to develop advanced construction materials based on the waste valorisation. As a result, building materials with self-healing and self-monitoring properties have been developed using electrically conductive metallic waste. Nevertheless, the addition of metallic waste may influence the electrical and thermal performance of the new building materials. This paper aims to evaluate the effect of the type and content of metallic waste (steel fibres and steel shavings) on the volumetric, electrical, and thermal properties of cement-based mortars designed with self-monitoring purposes. Physical, electrical, and thermal properties of cement-based mortars with four different contents of metallic waste were evaluated by measuring their bulk density, porosity, electrical resistivity, and thermal conductivity. In addition, metallic waste distribution inside the mortar specimens was measured by ultrasonic tests. All the properties were measured on specimens at two curing ages, 7 and 28 days. The main results showed that the addition of metallic waste produced a reduction of the bulk density and an increase of the porosity of cement-based mortars. Furthermore, it was proven that it is possible to evaluate the metallic waste distribution inside the mortars by ultrasound, and that this evaluation is more effective in specimens with fibres than in those with shavings. Likewise, it was proven that metallic waste can modify the electrical resistivity and the thermal conductivity of mortars, regardless of the type and amount of metallic waste. Finally, it was concluded that both the type and amount of metallic waste, and the curing time used in this research did not present a significant influence on the variation of the electrical resistivity and thermal conductivity of the evaluated cement-based mortars.

1. Introduction

Cement-based mortars are construction materials composed of cement, fine aggregates, and water. These composite materials are widely used in civil engineering due to their physical, mechanical, and thermal properties (Mindess et al., 2002). Nevertheless, the adverse environmental conditions, such as: freeze-thaw cycling (Cao and Chung, 2002), sulphates attack (Zhutovsky and Hooton, 2017), and contact with acids (Koenig and Dehn, 2016), combined with the external loads (Çavdar, 2014) can produce a reduction in their durability over time. With the aim of improving the mechanical resistance and durability of cement-based materials, different reinforcement additives (Brandt, 2008) such as crushed particles or fibres (Yoo et al., 2013) can be added to the cement-matrix (Bentur and Mindess, 2007). Some of these types of reinforcements are natural fibres (Pacheco-Torgal and Jalali, 2011), carbon fibres (Norambuena-Contreras et al., 2016), synthetic fibres (Quadir et al., 2016) and metallic fibres (Martinelli et al., 2015; Sengul, 2016).

Nonetheless, because of the high cost of commercial fibres and the need to dispose of solid waste from industrial sources, several studies have been carried out in recent years with the aim of developing innovative cement-based materials with advanced properties (Kim et al., 2014) by means of the valorisation of waste

* Corresponding author.
E-mail address: jnorambuena@ubiobio.cl (J. Norambuena-Contreras).

https://doi.org/10.1016/j.jclepro.2018.04.176

(Nagy et al., 2015). With this purpose, authors such as Chung (2012), Meehan et al. (2010) and Nguyen et al. (2015) focused on developing advanced cement-based materials with crack self-monitoring properties through the addition of electrically conductive fibres to the cement matrix and the measurement of electrical resistance variations in the composite material, as a physical indicator of material damage by cracking. Additionally, other studies have evaluated the use of metallic waste to develop cement-based materials with self-healing (Kim et al., 2014) and thermal-energetic (Corinaldesi et al., 2011) purposes with applications in industrial floors (Nagy et al., 2015) and thermo-solar plants (Girardi et al., 2017).

Furthermore, considering that the addition of metallic waste may also modify other properties of the cement-based materials, several studies have analysed the influence of solid waste on the physico-mechanical, thermal, and electrical properties of cement-based materials. For instance, Norambuena-Contreras et al. (2016) evaluated the effect of the addition of carbon powder waste on the physical and mechanical properties of cement pastes, resulting in a decrease in the bulk density and an increase in the porosity of materials, also affecting their mechanical properties. Nagy et al. (2015) compared the use of metallic and synthetic fibres in concrete, concluding that concrete with steel fibres presented higher values of bulk density and thermal conductivity than concrete with synthetic fibres. Similar results were reported by Corinaldesi et al. (2011) evaluating cement-based mortars but reinforced with rubber particles as waste.

On the other hand, Girardi et al. (2017) found that the thermal conductivity of concrete reinforced with metallic waste was double that of the reference material when adding a volume of 1% of waste. Khaliq and Kodur (2011) studied the influence of the fibre typology and the temperature on the thermal properties of concrete. Adding fibres of polypropylene, steel, or both, they concluded that steel fibres increased the thermal conductivity, while polypropylene fibres reduced it. Banthia et al. (1992) analysed the influence of the content of carbon and steel fibres on the variation of the electrical resistivity of cement pastes, concluding that the higher the percentage of fibres added, the lower the registered electrical resistivity. In this context, Lataste et al. (2008) and Solgaard et al. (2014) concluded that the variation of the electrical properties of cement-based materials with metallic fibres depends on the amount and morphology of the added fibres, and also on their physico-mechanical properties and distribution inside the material.

The current literature has identified some effects of the metallic waste on the cement-based materials. Nevertheless, there are still many open research questions that need to be addressed with the aim of understanding the phenomena associated with cement-based materials containing recycled metallic waste. For example, the effect on the properties of cement-based mortars of adding more than one type of metallic waste is not yet clear. Another less researched area concerns the optimum contents and types of metallic waste to yield cement-based composites with crack self-monitoring properties.

This paper has been prepared in the frame of a research project focused on the development of advanced cement-based mortars with crack self-monitoring purposes by the electrical conductivity control through the material. For this reason, electrically conductive metallic waste was mixed into the cement-based mortar. The main objective of this paper is to evaluate the influence of the type and amount of metallic waste on the volumetric, electrical, and thermal properties of cement-based mortars. To this end, nine different cement-based mortars with the same water/cement ratio but with two different types of metallic waste (steel fibres and steel shavings) added in four different contents (ranging from 4% to 16% by cement weight), were manufactured and evaluated at two different curing times (7 and 28 days).

2. Materials and methods

2.1. Materials

The raw materials used for the manufacturing of cement-based mortars were: Portland-Pozzolana Cement type IP (ASTM C595/C595M-16) with density 3.09 g/cm^3, fine sand (size between 0.15 and 2.0 mm) with density 2.81 g/cm^3, and a polymer synthetic-based superplasticiser with density 1.08 g/cm^3 (from Sika S.A. Chile). Gradation (ASTM C33-07) and physical properties (ASTM C128-01) measured for the fine sand used are shown in Table 1. Additionally, two electrically conductive types of metallic waste from industrial sources were mechanically cut and added to the cement-based mortars: steel wool fibres (Fig. 1(a)) and steel shavings (Fig. 1(b)). Steel fibres were composed of low-carbon steel, with a density of 7.180 g/cm^3 and an average electrical resistivity of 2.23×10^{-5} Ωm. These fibres had an average diameter of 0.133 mm (Fig. 1(c)), with an average aspect ratio of 44 and an initial length range of 2–14 mm, which means that both short and long fibres were added to the cement-based mortars. Similarly, steel shavings added to the mortars were formed of ferritic stainless steel, with a density of 7.980 g/cm^3 and an average electrical resistivity of 1.67×10^{-5} Ωm. These shavings had an average width of 1.310 mm (Fig. 1(d)) and an initial length within the range of 3–21 mm, which means that both short and long shavings coexist, resulting in four different types of geometry, see Fig. 1(b).

2.2. Preparation of test specimens

Table 2 presents the proportions by weight and volume of the raw materials used in this study. Cement-based mortar specimens were composed of cement, water, superplasticiser additive, and four different metallic waste amounts: 4%, 8%, 12% and 16% by unit weight of cement. These amounts of metallic waste were chosen in order to avoid difficulties during the mixing process and to achieve a good distribution. A water/cement ratio by weight of 0.5 was set for all the mortar mixtures with the aim of obtaining a normal consistency according to EN 196-3:2005 + A1:2009. Raw materials were mixed using a standard laboratory planetary mixer, adding the materials in the following order: first the cement and fine sand; second the water with the superplasticiser additive; and, finally, the metallic waste, when applicable. The mixing and manufacturing methodologies of the cement-based mortar specimens were as follows:

- First, cement and sand were mixed under dry conditions for 60 s at 75 rpm. At the same time, water and additive were

Table 1
Gradation and physical properties of the sand.

Sieve size (mm)	% Passing
2	100
1.18	92
0.6	71
0.3	9
0.15	0
Physical property	**Value**
Fineness modulus (−)	2.28
Bulk density (g/cm^3)	2.810
Specific gravity (−)	2.920
Water absorption (%)	1.4
Specific surface (cm^2/g)	17.84

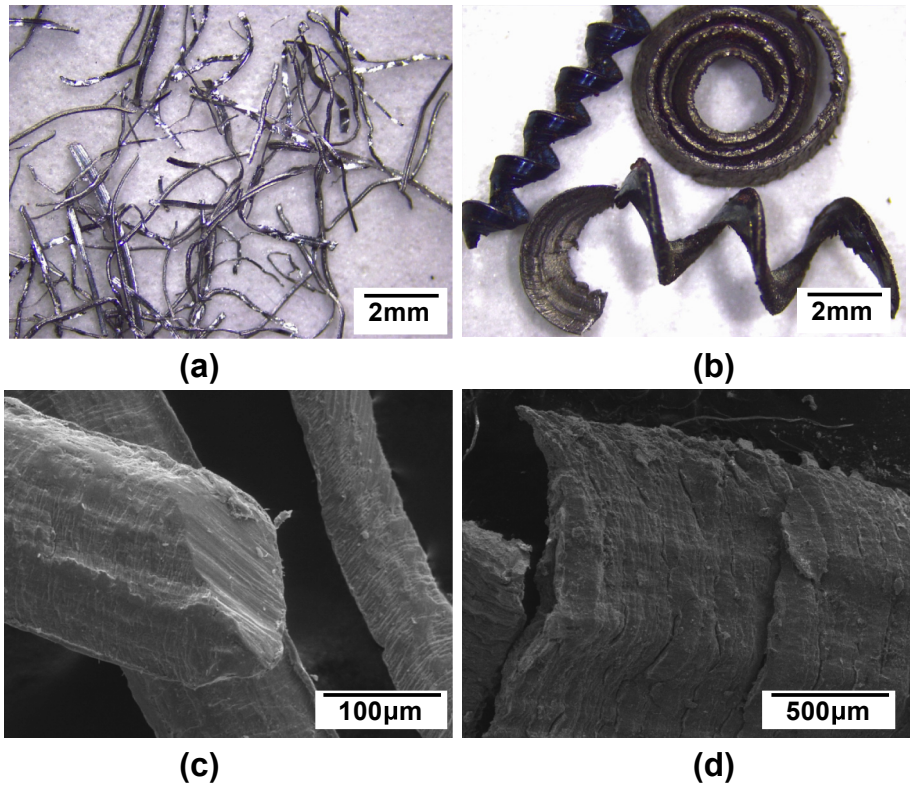

Fig. 1. Optical images (a–b) and SEM images (c–d) of steel wool fibres and steel shavings used.

Table 2
Proportions in weight and volume of the raw materials used in the cement mortars manufacture.

w/c ratio	Cement weight (g)	Sand weight (g)	Water weight (g)	Additive volume (cm^3)	Fibres and shavings amount (% by weight/ cement)	Weight of fibres and shavings (g)
0.5	450	1350	225	4.2	0	0
					4	18
					8	36
					12	54
					16	72

manually mixed in a separate bowl. Then, water with additive was added to the mixer and mixed at 75 rpm and 150 rpm for 60s and 60s, respectively.

- After that, the mix rested for 120s, and then the process finished with 60s of mixing at 150 rpm. In cases when metallic waste were added to the mortar, they were gradually incorporated while mixing at 75 rpm in order to avoid clusters. Then, the reinforced mortar mixture was mixed at 75 rpm for 120s.
- After the mixing process, the cement-mortar mixtures with, and without, metallic waste were poured into the prismatic moulds ($40 \times 40 \times 160$ mm) from one end of the specimens to the other end using a wide scoop. The specimens were slightly vibrated for 5s to minimise the presence of air bubbles inside them.
- Following the casting and compaction procedures, the prismatic moulds were covered with acetate sheets and placed in the laboratory, at ambient conditions, for 24 h to set, prior to demoulding.
- After demoulding, the cement-based mortar specimens were cured in a water tank in a standard controlled atmosphere at $22 \pm 5\ ^{\circ}C$ and $97 \pm 2\%$ humidity for two different curing times, 7 and 28 days.

Finally, a total of 216 prismatic test specimens were manufactured. A total of 192 specimens contained waste steel fibres and shavings while 24 reference specimens did not incorporate any metallic waste.

2.3. Chemical characterisation of raw materials

Raw materials used to manufacture the cement-based mortars were chemically characterised by elemental microanalysis and oxide content using energy dispersive X-ray spectroscopy (EDXS) and X-ray fluorescence (XRF). Basic element contents in the metallic waste were measured by EDXS characterisation using a Scanning Electron Microscope, TESCAN Vega-3 LMU, with an energy dispersive X-ray microanalysis unit incorporated. Additionally, oxide contents were measured by XRF characterisation in the cement and sand using an ARL Advant XP X-ray fluorescence spectrometer equipped with proportional flow and scintillation detectors. The chemical compositions of the cement and sand are shown in Table 3, while the basic elemental analysis of the metallic waste is shown in Table 4.

2.4. Morphological characterisation of metallic waste

To determine the morphological characteristics of the metallic

Table 3
Oxide chemical composition measured by XRF for the Portland-Pozzolana cement and fine sand used in the study. The uncertainty associated with the measurements was less than 1%.

Oxide type/amount (wt%)	SiO_2	Al_2O_3	Fe_2O_3	MgO	CaO	Na_2O	K_2O	SO_3	TiO_2	Sum
Portland-Pozzolana Cement	25.95	14.41	5.39	2.76	40.56	2.45	1.34	2.31	0.53	95.69
Fine Sand	44.93	20.81	7.83	6.13	9.09	4.94	0.68	–	1.87	96.29

Table 4
Elemental analysis measured by EDXS for the recycled metallic waste used in the study. The uncertainty associated with the measurements was less than 1%.

Element type/amount (wt%)	Metallic waste type	
	Shavings	Fibres
Fe	97.49	98.38
Mn	1.44	1.30
Si	0.51	0.18
Cr	0.21	–
C	0.30	0.12
Sum	99.95	99.98

waste added to the cement-based mortars, approximately 120 fibres and shavings were randomly selected from all the waste stored for the manufacturing. The length and diameter of the steel wool fibres, and the length and width of steel shavings were determined by taking photographs under an optical microscope, Leica EZ4 with 35× magnification, and calculating each length, diameter, or width using an image processing software ImageJ® (see Fig. 1(a) and (b)). Thus, the morphological variables of fibres and shavings have been presented in frequency histograms with the aim of comparing their length, diameter, or width distributions. Also, in view of the different geometries of the steel shavings, their morphological variables were also classified and measured according to the typology, see Fig. 2. In this way, it was possible to measure the contribution of each type of steel shaving in the specific frequency histogram. Finally, surface aspect and cross-section of steel wool fibres and steel shavings (either alone or embedded in cement-based mortar matrix) were analysed through SEM images obtained using a Scanning Electron Microscope, TESCAN Vega-3 LMU.

2.5. Bulk density and porosity of the test specimens

In order to evaluate the effect of the type and content of recycled metallic waste on the physical properties of the cement-based mortars after 7 and 28 days, bulk density (ρ) and water accessible porosity (n) of each test specimen with, and without, metallic waste have been measured and determined by equations (1) and (2) according to the standard ASTM C642-13. Finally, the representative densities and porosities of each cement-based mortar mixture have been determined as the average value of 12 specimens without metallic waste, and 24 specimens with metallic waste, for each curing time.

$$\rho = \frac{m_{dry}}{m_{sat} - m_{sub}} \cdot \rho_w \tag{1}$$

$$n = \frac{m_{sat} - m_{dry}}{m_{sat} - m_{sub}} \tag{2}$$

where m_{sat} is the water-saturated mass of the test specimens; m_{sub} is the water-submerged mass of the test specimens; m_{dry} is the oven-dried mass of the test specimens and ρ_w is the water density at testing temperature, as defined in the used method.

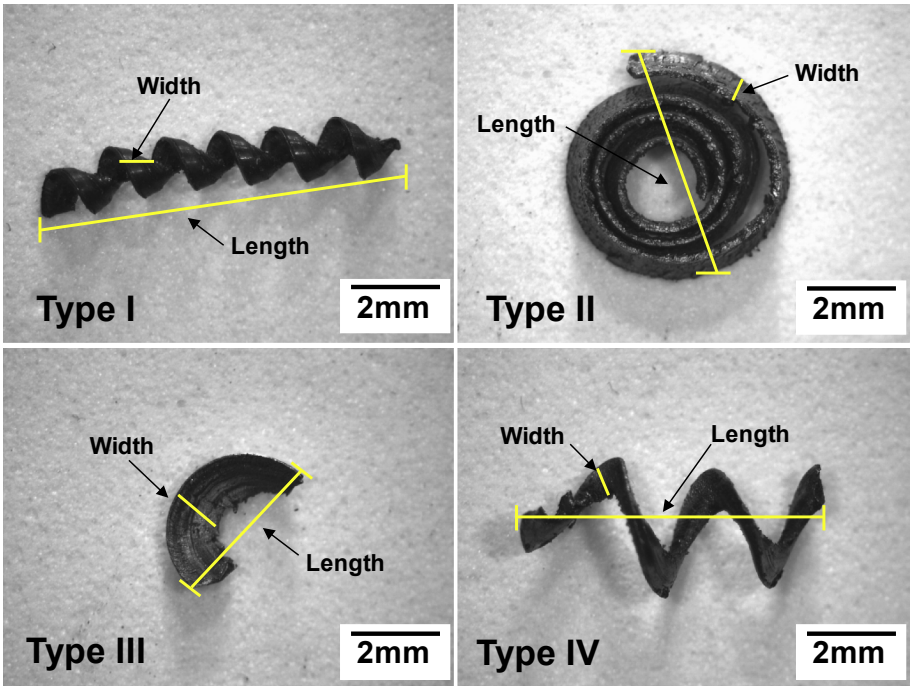

Fig. 2. Typology of the steel shavings used: measurement of the length and width.

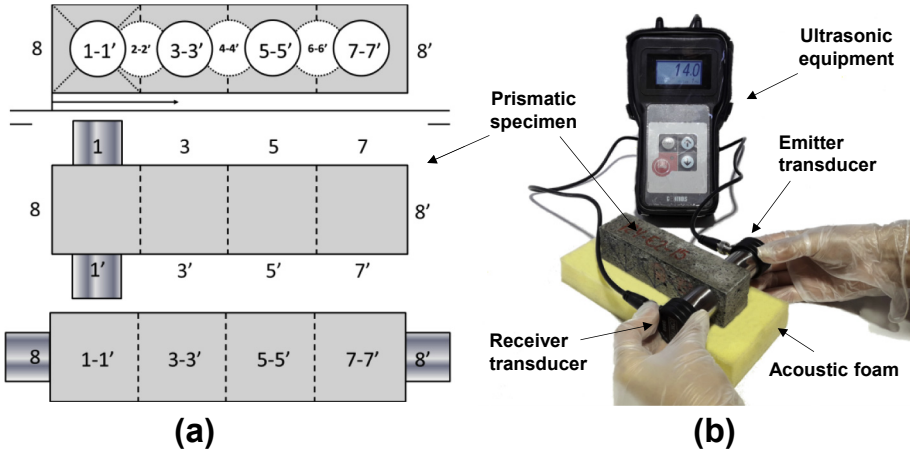

Fig. 3. (a) Measurement points on the prismatic test specimens; (b) Equipment and ultrasonic direct test set-up.

2.6. Evaluation of the metallic waste distribution inside the specimens by ultrasonic tests

With the aim of evaluating the metallic waste distribution inside the cement-based mortars after 7 and 28 days, the ultrasonic pulse time through the prismatic test specimens with, and without, metallic waste was measured. All the tests on specimens were developed by using ultrasonic direct tests based on the recommendations of Norambuena-Contreras et al. (2010). The ultrasonic test consisted of applying a high frequency compression pulse on the opposite faces of the prismatic specimens using an electro-acoustic transmitter. To do this, ultrasonic equipment, model 58-E4800 UPV (Controls Group) with 2 piezoelectric transducers of 54 kHz, was used (see Fig. 3). Additionally, petroleum jelly was used to ensure good contact between the transducers and the test specimen faces. To perform the tests in order to evaluate the metallic waste distribution inside the cement-based mortars, each test specimen was placed on an acoustic foam support and measured at 7 points across its thickness, thus evaluating the total of the prismatic specimen length (see Fig. 3(a) and (b)). In addition, all test specimens were tested along their length, see Fig. 3(a). In this way, the equipment determined the ultrasonic pulse propagation time for each point of the specimen, measured in microseconds (μs). The representative value of the propagation time at each point was calculated as the average of three repetitions of the measurement at the same point. Thus, higher ultrasonic pulse times in a specimen with metallic waste may imply a higher porosity of the material (zones with lower density) or the presence of less metallic waste. In contrast, lower propagation times can be associated with low porosity (high density zones) or with a high presence of metallic waste.

2.7. Measurement of electrical resistivity of the test specimens

To evaluate the influence of the type and amount of metallic waste on the electrical resistivity of the cement-based mortars after 7 and 28 days, the electrical resistance of all the prismatic test specimens with, and without, metallic waste has been measured, see Fig. 4. An ohmmeter, model HIOKI IR4056-20, connected to two stainless steel plate electrodes with dimensions 10 × 15 cm, was used. Thus, each electrode was placed on the opposite faces of the prismatic specimen, ensuring that the specimens were centred, and the electrode plates aligned. Moreover, to guarantee a better contact between the electrode and the specimen surface, a small pressure of 1 kPa was applied on the electrodes. This allowed stable values of electrical resistance to be obtained for each measurement.

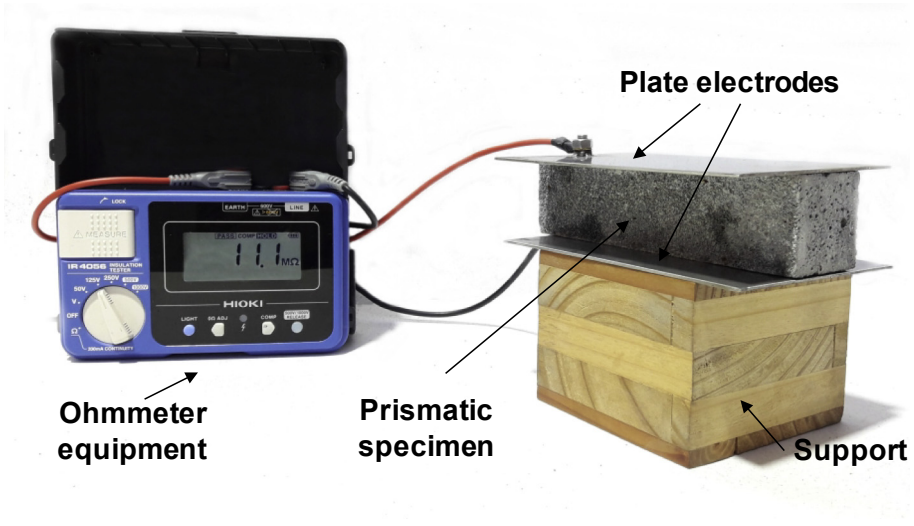

Fig. 4. Measurement of the electrical resistance on the prismatic test specimens of cement mortars.

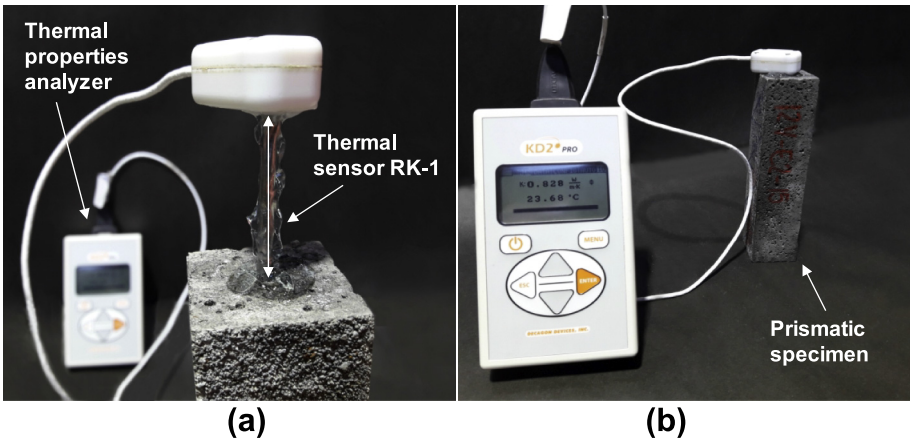

Fig. 5. (a) Handheld controller and thermal sensor; (b) measurement of the thermal conductivity.

Hence, after measuring the electrical resistance of each specimen, the electrical resistivity was obtained according to the second Ohm's law, as shown in Equation (3):

$$\rho = \frac{R \cdot S}{l} \tag{3}$$

where R is the electrical resistance of each test specimen, measured in Ω; S is the area of the plate electrodes, measured in m^2; and l is the thickness of each test specimen, measured in m. The electrical resistivity representative of each tested specimen was determined as the average value of 3 repetitions.

2.8. Measurement of thermal conductivity of the test specimens

To evaluate the influence of the type and amount of metallic waste on the heat transfer ability of the cement-based mortars after 7 and 28 days, the thermal conductivity of all prismatic test specimens with, and without, metallic waste has been measured using the thermal needle probe method. This method is based on the transient linear heat source theory according to the standard ASTM D 5334. To do this, a KD2-Pro thermal properties analyser from Decagon Devices Inc. was used, comprising a handheld controller and a thermal sensor (see Fig. 5). In this research, a needle RK-1 sensor (length 60 mm and diameter 3.9 mm) with a measurement range of 0.1–6.0 W/mK was used. The following steps were followed to perform the tests: first, the thermal sensor was covered with a polysynthetic thermal compound that reduces the presence of air voids and the contact resistance between the sensor and the internal surface of the specimen. Then, the sensor was embedded in the previously drilled specimen, see Fig. 5(a). The heat generated by the RK-1 sensor inside the specimen creates a temperature gradient, which is detected by the needle sensor and recorded by the testing equipment, see Fig. 5(b). Each test had a total duration of 10 min. Finally, the thermal conductivity (λ) of each test specimen was calculated using Equations (4) and (5) (Wang et al., 2016):

$$T = m_1 + m_2 \cdot t + m_3 \cdot ln(t) \tag{4}$$

where T is the recorded temperature; m_1 is the environmental temperature during heating; m_2 is the varying rate of background temperature; m_3 is the slope of a line relating temperature rise to logarithm of temperature; and t is the testing time.

$$\lambda = \frac{q}{4 \cdot \pi \cdot m_3} \tag{5}$$

where λ is the thermal conductivity measured in W/mK; and q is the heat generated by the sensor in W/m. The thermal conductivity of each test specimen was determined as the average value of 3 measurements.

2.9. Experimental variables evaluated in the study

Table 5 presents the abbreviations of the variables included in this study. 11 variables in total have been analysed. Four variables concern the characteristics of the metallic waste: diameter and length of the steel wool fibres, and length and width of the steel shavings. Five are related to the physical properties of the cement-based mortars: percentages of metallic waste, curing time, bulk density, porosity, and ultrasonic pulse time of the cement-based mortars. And two variables concern the electrical and thermal

Table 5
Variables included in the experimental study.

Classification	Name	Abbreviation	Unit
1. Characteristics of the recycled metallic waste	Diameter of fibres	*DF*	mm
	Length of fibres	*LF*	mm
	Width of shavings	*WS*	mm
	Length of shavings	*LS*	mm
2. Physical properties of the mortars	Percentages of waste	*PW*	%
	Curing time	*CA*	days
	Bulk density	*BD*	g/cm^3
	Porosity	*n*	%
	Ultrasonic time	*UT*	μs
3. Electrical and thermal properties of the mortars	Electrical resistivity	*ER*	Ω·m
	Thermal conductivity	*TC*	W/mK

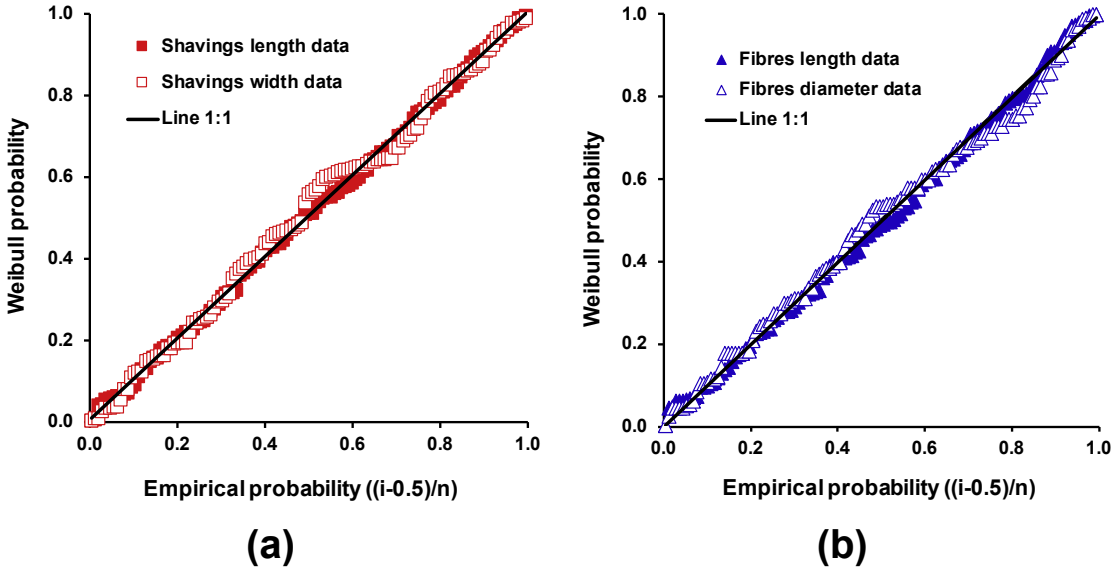

Fig. 6. Weibull probability-probability plot of the (a) length and width of the metallic shavings, and (b) length and diameter of metallic fibres.

properties of the cement-based mortars: electrical resistivity and thermal conductivity, respectively.

3. Results and discussion

3.1. Analysis of the morphology of mechanically cut metallic waste

To ensure a good distribution and embedding of the metallic waste inside the cement-based mortar mixtures, fibres and shavings must have some optimum morphological properties. With this in mind, both steel fibres and steel shavings were mechanically cut and sieved to facilitate the mixing and compaction process of the raw materials, thus obtaining an improvement in their workability and distribution inside the cement-based mortar matrix. With the aim of proving that the morphological properties of mechanically cut fibres and shavings follow a probability law, a probability analysis has been developed on all morphological results measured, such as: length and diameter of steel wool fibres, and length and width of steel shavings. In this way, all the fibres and shavings, regardless of their original morphological properties, have been represented together by fitting a Weibull probability distribution function, see Fig. 6(a) and Fig. 6(b), respectively. From these Figures, a good data fitting can be considered due to the fact that all the morphological results, regardless of the original metallic waste type, can be aligned in a 1:1 straight line. This result is similar to those reported in previous studies about the morphological characterisation of recycled metallic fibres (Norambuena-Contreras et al., 2015) and crushed polyethylene particles (Norambuena-Contreras et al., 2017) used to design new composite materials.

Moreover, the Weibull probability distribution function has been used in this analysis as a material damage function (Norambuena-Contreras et al., 2016), considering that the cutting action on fibres and shavings occurs due to many small cuts that happen during each specific industrial cutting process, such as longitudinal cutting for fibres and turning for shavings. Furthermore, with the aim of knowing the occurrence probability of the morphological studied variables, the frequency histograms for all the data measured, using an optical microscope, have been

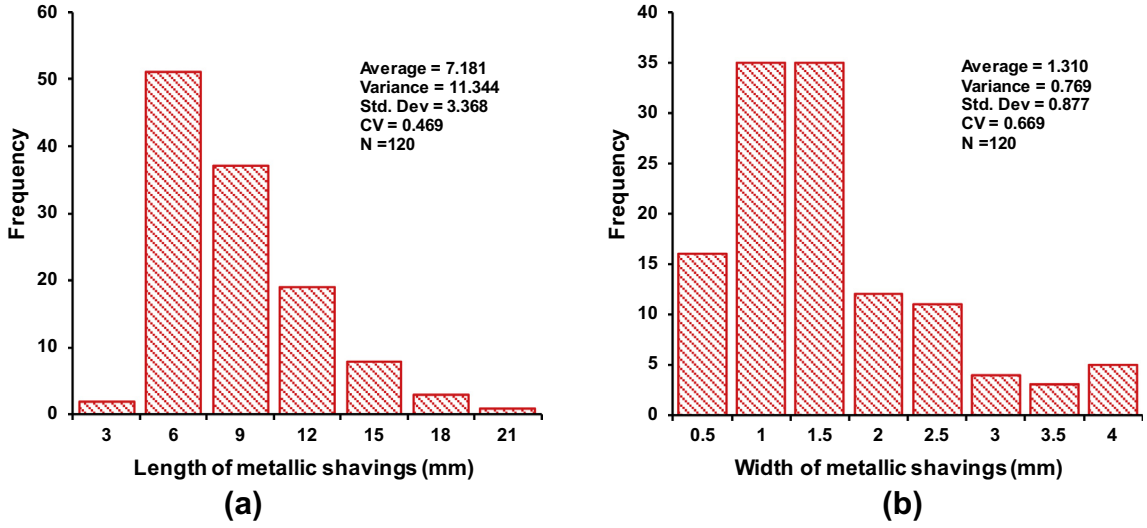

Fig. 7. Frequency histograms based on the Weibull probability function for the shavings (a) length, and (b) width.

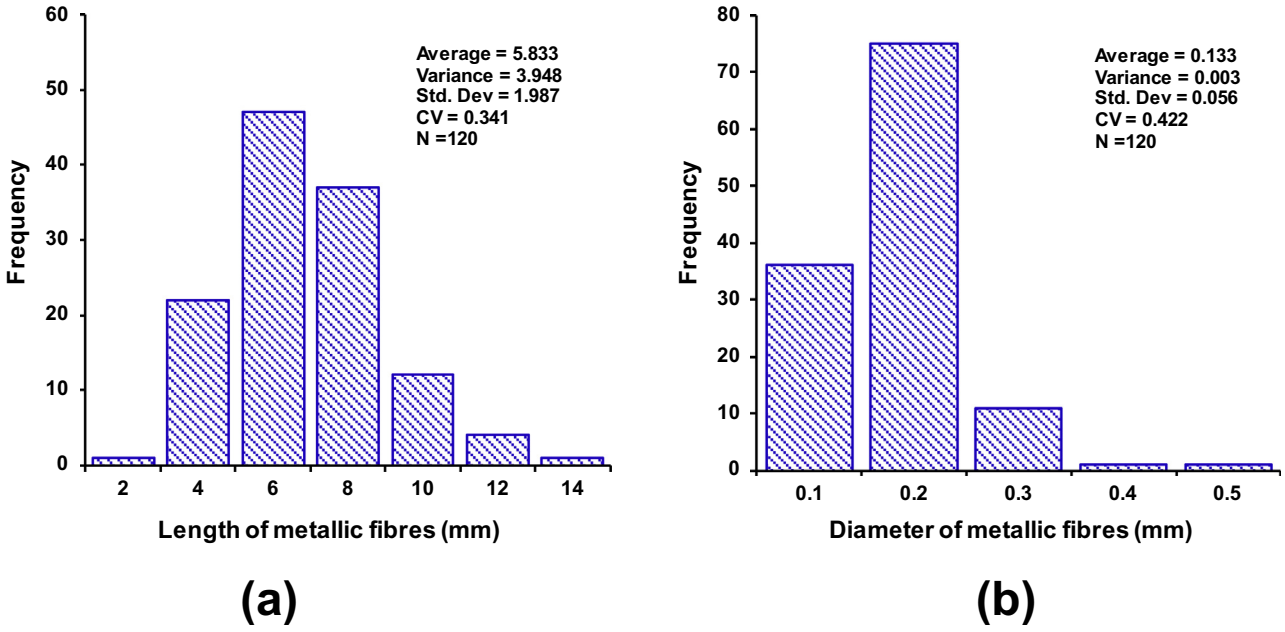

Fig. 8. Frequency histograms based on the Weibull probability function for the fibres (a) length, and (b) diameter.

represented in Fig. 7 and Fig. 8. Based on these histograms, it was proven that the steel shavings (average length 7.181 mm) are on average longer than the steel wool fibres (average length 5.833 mm), see Figs. 7(a) and Figure 8(a), respectively. Likewise, it was proven that the width of the steel shavings is 10 times higher than the diameter of the fibres, as can be seen in Figs. 7(b) and Figure 8(b). However, this result may be influenced by the morphology of the steel shavings used, see Fig. 1(b). In this study, four different types of steel shavings have been identified, with different lengths and widths, see Fig. 2.

Table 6 presents the proportion represented by each type of shaving on the total amount of shavings shown in Fig. 7, and their average length and width. In this Table, it can be observed that the largest amount of shavings is Type III (47%), followed by Type IV, I, and II, with amounts of 24%, 22%, and 7%, respectively. Additionally, the longest shavings are Type IV (average length 9.38 mm) and Type I (average length 8.43 mm), followed by Types II and III, with average lengths of 5.78 and 5.67 mm, respectively. Moreover, the shavings that presented the highest width were Type III, with average value of 1.83 mm. These results are consistent compared to Fig. 7, which demonstrates that, regardless of the amount of shavings added to the cement-mortar mixtures, there is a 88% probability that the shavings are long, ranged from 6 to 12 mm (see Fig. 7(a)), with a 71% probability that the width ranged from 0.5 to 1.5 mm, and 20% probability that it ranged from 2 to 2.5 mm (see Fig. 7(b)).

On the other hand, from Fig. 8, it was demonstrated that, regardless of the amount of fibres added to the mortar-cement mixtures, there is 85% probability of having long fibres, between 4 and 8 mm. At the same time, the probability of adding shorter (under 4 mm) or longer (over 8 mm) fibres is much lower, being 1% and 14%, respectively. As a result, the length of the fibres ranged from 2 to 14 mm, with an average length of approximately 5.8 mm (see Fig. 8(a)). This value can be considered as a medium-length fibre according to the results published by Norambuena-Contreras et al. (2015). Finally, the diameter calculated from the measurement of 120 individual fibres by using an optical microscope was, on average, 0.133 mm (see Fig. 8(b)). This value can be considered as a thick type of fibre according to García et al. (2013). Overall, it can be concluded that long and thick fibres and shavings were added to the cement-based mortar mixtures.

Table 6
Length and width average of the steel shavings classified by typology.

Type of steel shavings according to Fig. 2	Proportion of shavings on total	Average length (mm)	Average width (mm)
I	22%	8.43	1.00
II	7%	5.78	0.99
III	47%	5.67	1.83
IV	24%	9.38	0.68

3.2. Influence of metallic waste on the physical properties of the test specimens

Fig. 9 shows the average results and standard deviation bars of the bulk density (Fig. 9(a)) and porosity (Fig. 9(b)) of the mortar specimens with different types and contents of metallic waste, evaluated at two curing times. In Fig. 9(a) it can be observed that, regardless of the type of metallic waste and curing time, the bulk density proportionally decreased with the increase of the amount of metallic waste. Thus, the highest average value of density was obtained in the case of reference specimens without metallic waste, 1.731 and 1.705 g/cm^3 at 7 and 28 days, respectively.

Additionally, the lowest average values of density were obtained in the case of mortars with 16% of metallic waste, obtaining 1.667 and 1.666 g/cm^3 for mortars with shavings, and 1.693 and 1.680 g/cm^3 for mortars with fibres, at 7 and 28 days, respectively. However, comparing the reduction rate in Fig. 9(a), it can be observed that mortars with shavings presented higher reductions in the bulk density than in the specimens with fibres. This difference was due to the morphology of the metallic waste used in the study, and to their influence on the volumetric properties of the mortar. Hence, the irregular shape of the shavings (see Fig. 2) caused a higher increase in the total volume of mortar specimens, compared to those with fibres (see Table 7), which have a more regular shape. This result was proven with both curing times. Additionally, it was demonstrated in this study that the bulk density of the mortars

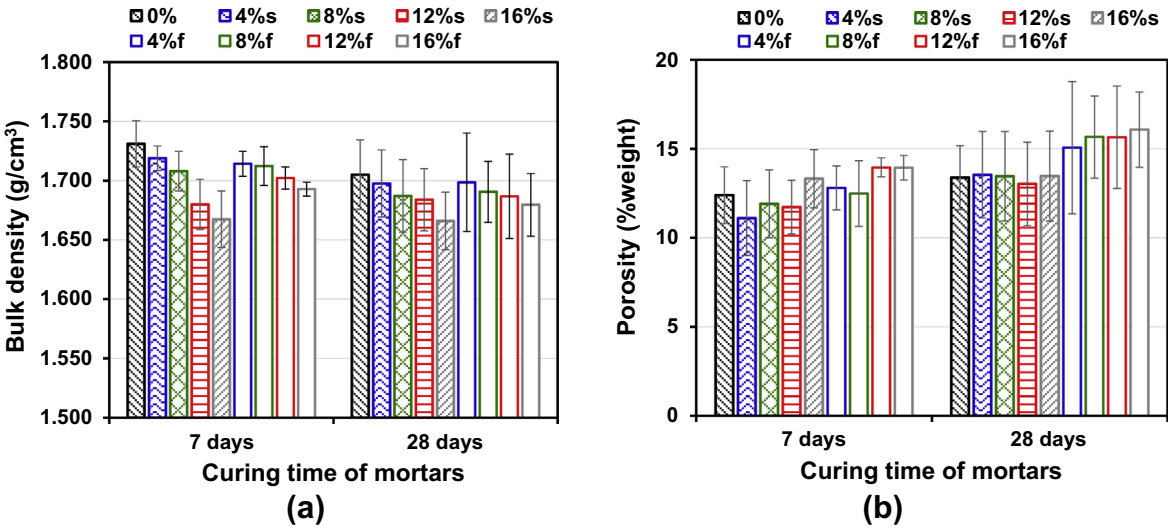

Fig. 9. Average results of the (a) bulk density and (b) porosity of the cement mortar specimens for the different waste content and curing times (s: shavings and f: steel wool fibres).

Table 7
Results of average volume in cm^3 measured on the prismatic specimens with and without shavings and fibres.

Metallic waste content	Metallic waste type and curing time			
	Shavings		Fibres	
	7 days	28 days	7 days	28 days
4%	308.0	308.8	302.1	301.9
8%	306.7	310.4	304.9	305.9
12%	320.2	313.3	304.4	305.3
16%	321.2	321.8	310.3	304.8
R0%	298.2	308.3	298.2	308.3

with metallic waste was also affected by the type of waste added. To prove this, Fig. 10 presents all the bulk density values obtained from the mortar specimens versus their porosity value. In this Figure, it can be observed that, regardless of the amount of metallic waste and the curing time, there is a linear relationship between porosity

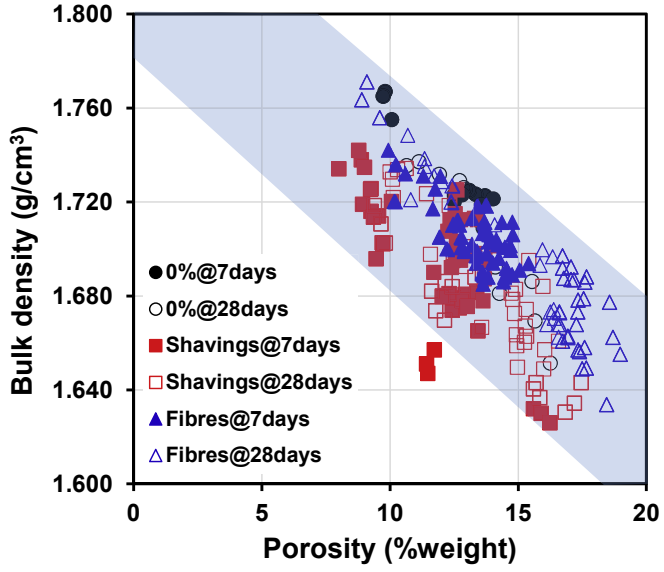

Fig. 10. Relationship between the bulk density and porosity of the cement mortar specimens.

and bulk density. In this context, the bulk density proportionally reduced with the increase of the porosity and, in general, specimens with fibres had higher density than specimens with shavings (see Fig. 10), comparing specimens with equivalent porosity. This result can also be seen in Fig. 9(a) comparing the density values obtained for both curing times, where specimens with fibres gave average density values higher than those obtained with specimens of mortar with shavings. Likewise, the results indicate that the average bulk density reduced with an increase of the curing time. However, observing the error bars of the density results in Fig. 9(a), this conclusion could be considered as not significant, considering the variability of the presented results. Therefore, this study cannot conclude that the curing time has a significant influence on the density of the mortar specimens. As result, it can be stated that the variation of the bulk density of mortars with metallic waste with respect to specimens without metallic waste was attributed more to the variation of the total volume of the specimens (Table 7) than to the variation of their dry mass.

Moreover, Fig. 9(b) shows that, in general, regardless of the curing time and the type of metallic waste, specimens with higher amounts of metallic waste present higher average porosity. During the measurements, it was observed that the lowest values of porosity were registered in the reference mortars without metallic waste. Also, comparing the average values of porosity, it was observed that the specimens with steel wool fibres presented higher porosities than the specimens with metallic shavings, both curing times, which is related to the elemental composition of the metallic waste, see Table 4 and Fig. 9(b). Thus, metallic fibres made with low-carbon steel (Fig. 1(a)) are more ductile than shavings, and consequently more susceptible to the formation of clusters during the mixing process. Specifically, the interconnection between the clusters resulted in a higher connection between the pores, which increased the content of pores accessible for water. In contrast, the stainless-steel shavings are stiffer and more fragile than the steel wool fibres due to their high content of carbon and chromium (see Fig. 1(b)), so they can break into smaller pieces during the mixing process and consequently, they can present a better distribution inside the mortars, being less likely to form clusters. Because of that, the lack of connection between the shavings means that the formation of pores around them does not result in an increase of the porosity accessible for water, but in a reduction of the mortar density. This can be seen by observing the

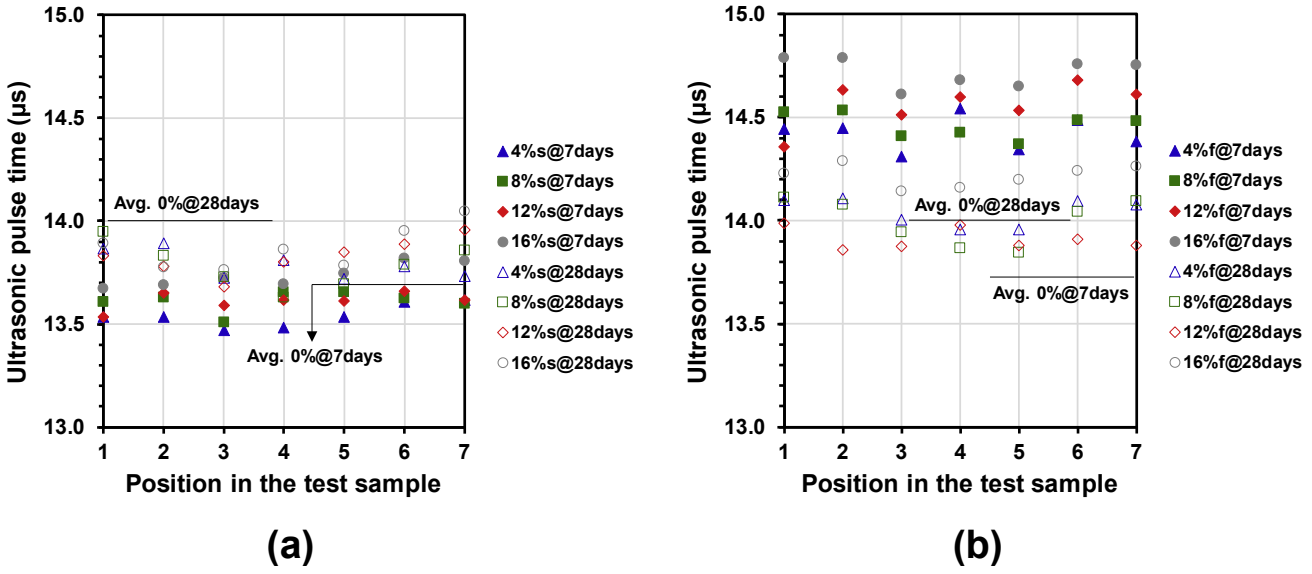

Fig. 11. Relationship between the average ultrasonic time and the test position for cement mortar specimens reinforced with (a) shavings and (b) steel wool fibres.

results of the ultrasonic pulse times measured for specimens with fibres, and with shavings, shown in Fig. 11 and Fig. 12. In addition, it was found in this study that the average porosity of the mortar specimens increased with an increase of the curing time, see Fig. 9(b). However, analysing the variability of the porosity results shown by the error bars in Fig. 9(b), it can be concluded that the variation is not significant. Therefore, as with the density, the curing time does not have a significant influence on the porosity of mortar specimens.

3.3. Analysis of metallic waste distribution inside the test specimens

Fig. 11 shows the results of the average ultrasonic pulse time obtained for the mortar specimens with different amounts of the two types of metallic waste and evaluated at two curing times. Thus, Fig. 11(a) and (b) show the ultrasonic pulse time results measured through the thickness of the mortar specimens at 7 different positions (see Fig. 3) for the specimens with shavings, and with fibres, respectively. The ultrasonic pulse time results can be qualitatively interpreted as the spatial distribution of the shavings and fibres inside the mortars (Norambuena-Contreras et al., 2015). Additionally, it can be observed in Fig. 11 that, regardless of the measurement position along the sample, average ultrasonic pulse times are in general slightly lower in the case of mortars with shavings than in mortars with fibres. This difference can be more clearly observed in Fig. 12(a), where the average values of ultrasonic pulse time are presented, independently of the measurement position. The error bars in this Figure correspond with the standard deviation value.

Moreover, Fig. 11 shows that the average ultrasonic pulse times obtained from the specimens with fibres gave more scattered values compared with those obtained from the specimens with shavings. Likewise, the highest values of ultrasonic pulse time were obtained at the extreme positions of the specimens (see positions 1

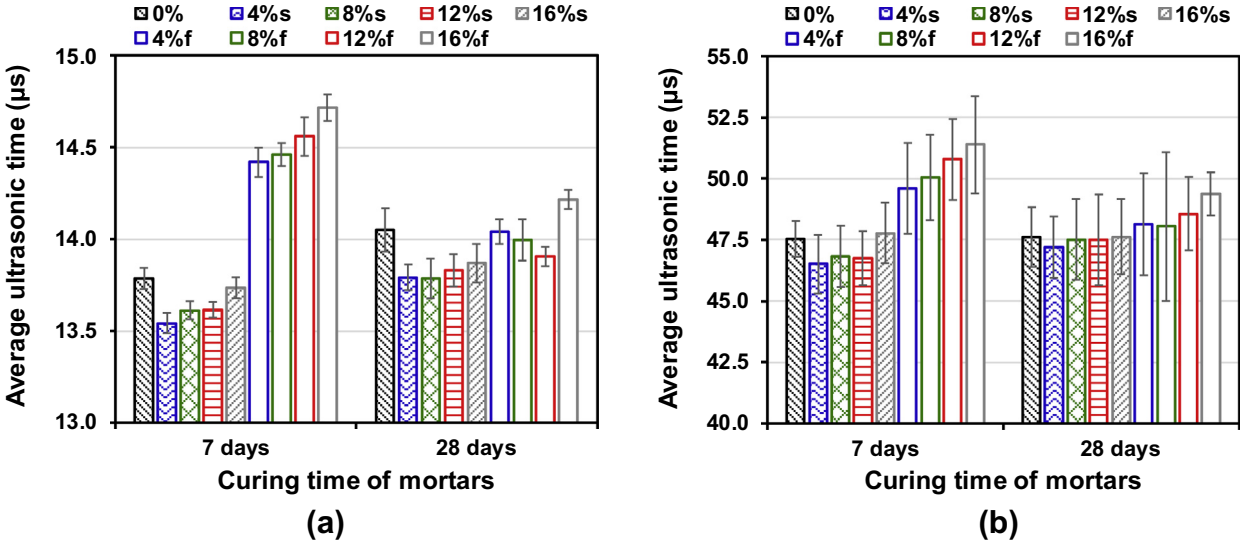

Fig. 12. Average ultrasonic time through the (a) thickness and (b) length of the cement mortar specimens for the different waste content and curing times (s: shavings and f: steel wool fibres).

and 7 in Fig. 11), while the lowest values of ultrasonic times were measured at the central positions (see positions 3–5 in Fig. 11), regardless of the type and amount of waste and the curing time. The lower ultrasonic pulse times can be indicative of the presence and high connectivity of metallic waste in the central zone of the mortar specimens, which can be due to the boundary conditions of the prismatic moulds and their influence during the compaction process of the mortars. In this way, the vibration process needed to compact the mortars results in the metallic waste materials, which are denser than the mortar matrix, moving and accumulating in the centre of the specimens.

With this in mind, in the specimens with shavings (see Figs. 11(a) and Figure 12(a)) the ultrasonic pulse times proportionally increased with the amount of shavings and the curing time. For example, in Fig. 11(a), the highest value of ultrasonic time (14.05 μs) corresponded to the specimens with 16% of shavings tested after 28 days of curing. Overall, specimens with shavings after 28 days of curing showed average ultrasonic times higher than the specimens after 7 days of curing, see Fig. 12(a). This can be due to the higher porosity values of the specimens at a curing time of 28 days (see Fig. 9(b)), which results in an increase of the air void content inside the mortars and consequently in an increase of the ultrasonic propagation time.

Additionally, it was observed that the specimens with steel wool fibres presented higher values of the ultrasonic average times than either the reference specimens without waste or the specimens with shavings, regardless of the amount of fibres and the curing time, see Figs. 11(b) and Figure 12(a). These results are coincident with those obtained in Fig. 9(b), where it can be seen that specimens with fibres presented, in general, higher porosity accessible for water than both the reference specimens and the specimens with shavings, resulting in a higher air void content together with a higher ultrasonic pulse time. However, based on the variability of the porosity results presented in Fig. 9(b), the influence of the porosity on the ultrasonic pulse time variation may be not significant for the evaluated specimens with shavings and fibres. Hence, the lower ultrasonic times obtained in specimens with shavings compared with those obtained in specimens with fibres (see Fig. 11) can be attributed to the higher density of shavings (10% higher than fibres), due to the fact that they have a higher content of constituent elements (Mn, Si, Cr and C) than the fibres, see elemental analysis in Table 4.

Furthermore, Fig. 12(b) shows the average ultrasonic pulse time measured along the mortar specimens (see Fig. 3). The error bars in this Figure correspond with the standard deviation of the results. It can be observed that the ultrasonic time results along the specimens presented a similar trend to those measured across them (Fig. 12(a)), but gave higher ultrasonic time values due to the distance between the transductors (4 times longer). Thus, the highest ultrasonic pulse times were registered in specimens with fibres after 7 days of curing, being reduced at the curing time of 28 days. However, based on the variability of the results (see error bars in Fig. 12(b)), the influence of the curing time may not be significant.

3.4. Influence of metallic waste on the electrical and thermal properties

Fig. 13 shows the average results of the electrical resistivity of cement-based mortars versus the amount of metallic waste. These results were presented in a semi-logarithmic graph, where the points represent the scatter of the results obtained for each content of metallic waste, and the continuous lines represent the average values at each curing time. In general, the electrical resistivity values were similar, regardless of the type and content of metallic waste. For example, in the case of mortar specimens with 8% of shavings, the registered average values were 8.64×10^6 and 1.03×10^7 Ωm, at curing times of 7 and 28 days respectively, which corresponds to a variation of 16%. A similar behaviour happened in the case of mortar specimens with fibres, where electrical resistivity values of 2.02×10^7 and 2.46×10^7 Ωm were obtained at curing times of 7 and 28 days, respectively, in mortars with 16% of fibres (Fig. 13(b)), which represents a variation of 18%. Thus, in the case of both shavings and fibres, average values of electrical resistivity are in a similar range, demonstrating that the curing time did not have a significant influence on the electrical resistivity of the specimens. However, during the measurements it was observed that the electrical resistivity decreased with the increase of the waste content. In this way, regardless of the type of metallic waste (shavings or fibres), it is possible to observe, in Fig. 13, that the reference specimens registered electrical resistivity values slightly higher than the specimens with metallic waste (average value of 3.95×10^7 and 1.10×10^7 Ωm, at curing times of 7 and 28 days, respectively). So, the addition of metallic shavings and fibres, regardless of the amount, caused a decrease in the resistivity and an

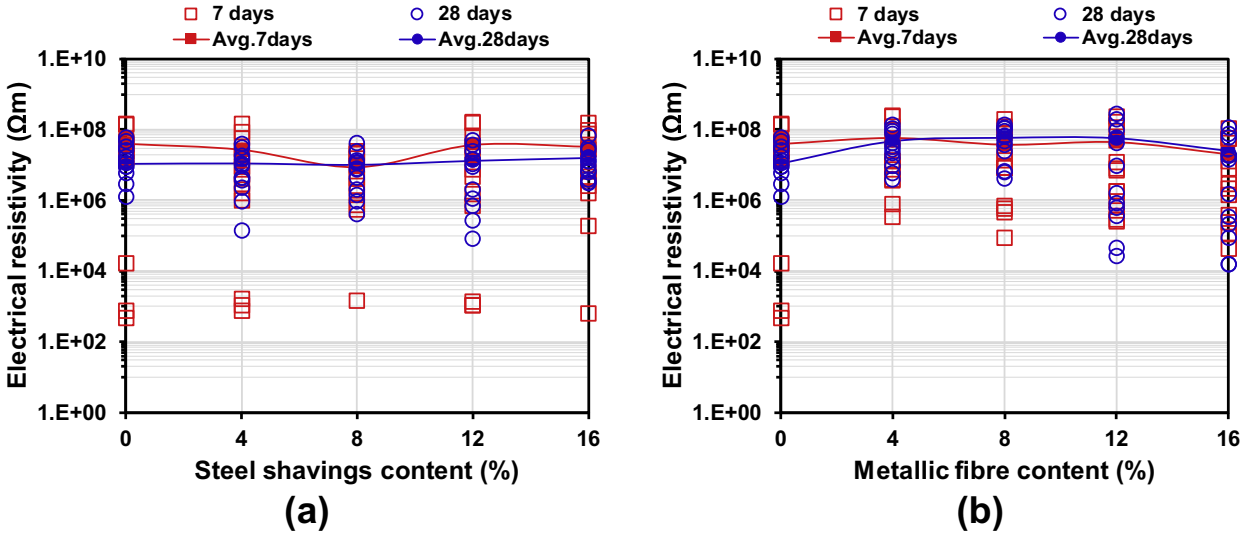

Fig. 13. Relationship between the electrical resistivity and the metallic waste content for cement mortar specimens reinforced with (a) shavings and (b) steel wool fibres.

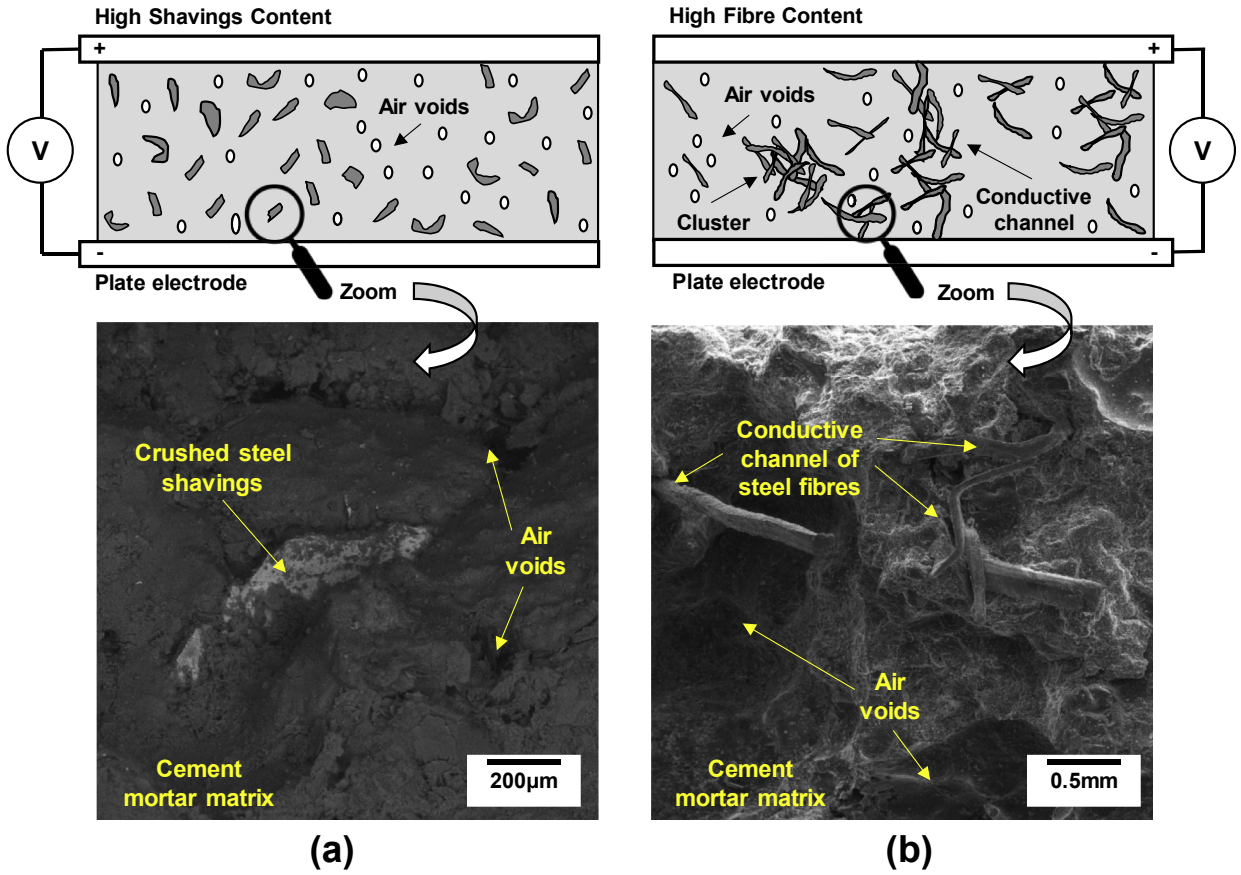

Fig. 14. Scheme of the electrical resistivity measurement. Influence of the type and content of metallic waste inside of cement mortar specimens reinforced with (a) shavings and (b) steel wool fibres.

increase in the electrical conductivity of the mortars by a similar order of magnitude (see continuous lines in Fig. 13), even though their elemental composition and morphological characteristics are different.

With the aim of clarifying this behaviour, Fig. 14 shows a schematic representation of the influence of the type and content of metallic waste inside the mortars during the electrical resistivity measurement, with the addition of SEM images of the shavings and fibres embedded in the cement-based mortar matrix. In this Figure, it can be seen that the shavings were crushed during the mixing process, resulting in shorter particles that can be better distributed in the mortar matrix (see Fig. 14(a)). In contrast, since the fibres are longer and more flexible than the shavings, they can form fibre clusters and consequently conductive channels along them, see Fig. 14(b). Therefore, it can be concluded that the fibres balance their low electrical conductivity inside the mortars (25% lower than metallic shavings) with the fact that they are able to interconnect, forming conductive channels, while the shavings cannot interconnect. However, although the fibres presented a slight reduction in the average electrical resistivity with the increase of the content added to the mortar (Fig. 13(b)), this reduction cannot be adjusted to a percolation model (Xie et al., 1996), leading to the conclusion that the mortar with fibres did not present an electrically conductive behaviour.

On the other hand, Fig. 15(a) and (b) show the average results of the thermal conductivity measurements depending on the metallic waste content. In these Figures, the points represent the scatter of the results, and the continuous lines represent the average values at each curing time, as in the previous case. The results obtained from the mortars with shavings (Fig. 15(a)) show that, in general, the reference specimens had an average thermal conductivity of 0.868 and 0.796 W m-1K^{-1} at curing times of 7 and 28 days, respectively, which was less than, or equal to, that obtained from the specimens with shavings. So, the addition of metallic shavings increased the thermal conductivity of the mortars at the curing time of 28 days and kept it constant at a curing time of 7 days. This behaviour was different in the case of mortars with fibres (see Fig. 15(b)), where the addition of metallic fibres produced a decrease in the thermal conductivity, regardless of the curing time.

Furthermore, comparing the thermal conductivity results between specimens with shavings (Fig. 15(a)) and fibres (Fig. 15(b)), it can be observed that the addition of metallic fibres produced a decrease in the average values of thermal conductivity, while the shavings increased, or kept constant, the thermal conductivity compared with specimens without metallic waste. In conclusion, the addition of steel wool fibres did not increase the heat transfer ability of the cement-based mortars. This result may be due to the porosity of the mortar specimens with metallic waste and its distribution inside them. With the purpose of demonstrating this, Fig. 16 presents the relationship between the thermal conductivity and the porosity of all the mortar specimens evaluated in the study. It can be observed that the higher the porosity is, the lower the measured thermal conductivity. As previously discussed, specimens with fibres studied in this research had higher porosity than specimens with shavings (Fig. 9(b)), due to the formation of clusters that have air inside (see SEM Image in Fig. 14(b)), thus increasing the total porosity of the mortars and reducing the heat transfer ability through them.

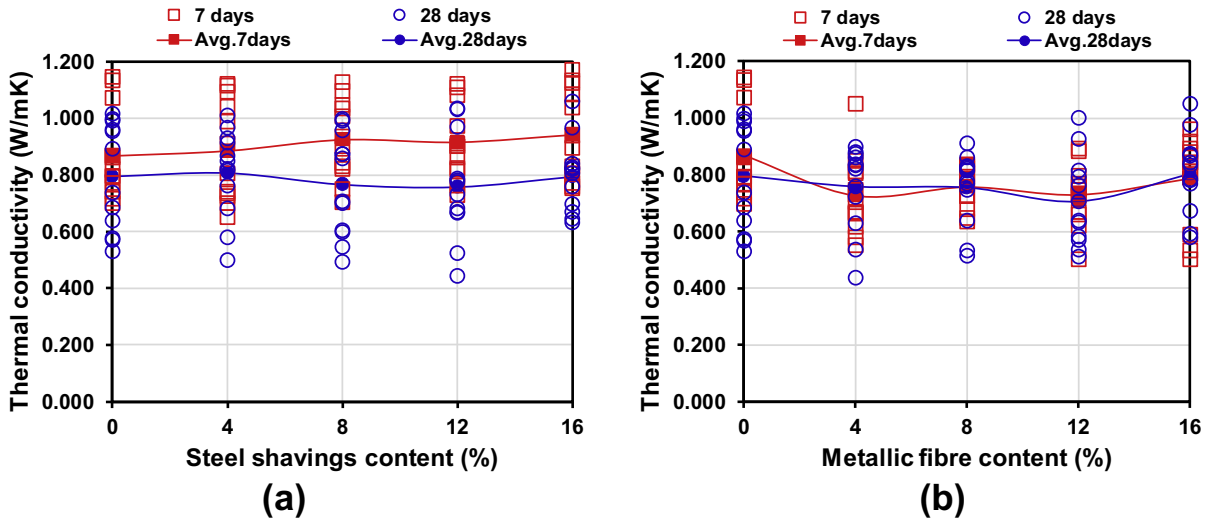

Fig. 15. Relationship between the thermal conductivity and the metallic waste content for cement mortar specimens reinforced with (a) shavings and (b) steel wool fibres.

In summary, analysing the obtained results of electrical resistivity (Fig. 13) and thermal conductivity (Fig. 15), it was observed that the type and content of waste, and curing time did not present a significant influence on the variation of the electrical and thermal conductivity, with respect to a reference mortar without metallic waste. With the aim of evaluating the influence of these variables on the electrical and thermal behaviour of the cement-based mortars, an evaluation RATIO was defined in this study, for each electrical and thermal property. This ratio has been defined as the quotient between the i-th value (V_i) of electrical or thermal conductivity from the mortar specimens with metallic waste, $(V_{i-with\ metallic\ waste})$, and the average value of the same property measured in specimens without metallic waste, $(V_{i-without\ metallic\ waste})$, evaluated at the same curing time, as follows:

$$RATIO = \frac{V_{i-with\ metallic\ waste}}{V_{i-without\ metallic\ waste}} \quad (6)$$

Consequently, to demonstrate the hypothesis that the studied variables do not have a significant influence on the variation of the electrical and thermal conductivity of mortars compared to mortars without metallic waste, Fig. 17 presents the P-P Plots for all the RATIO data of the tested specimens, represented using a Weibull probability distribution function. The RATIO data have been represented, regardless of the type and amount of metallic waste and the curing time. It can be observed that all results can be aligned to a straight line with a slope 1:1, which indicates that neither the type nor the amount of metallic waste, nor the curing time, present a significant influence on the variation of the studied properties in mortars evaluated under experimental conditions. Finally, the Weibull probability function was used in the study considering that the electrical resistivity and thermal conductivity values of the evaluated mortars are the result of the unpredictable nature of the contacts between shavings or fibres inside the specimens (Sevkat et al., 2008), due to the mixing and vibratory compaction processes.

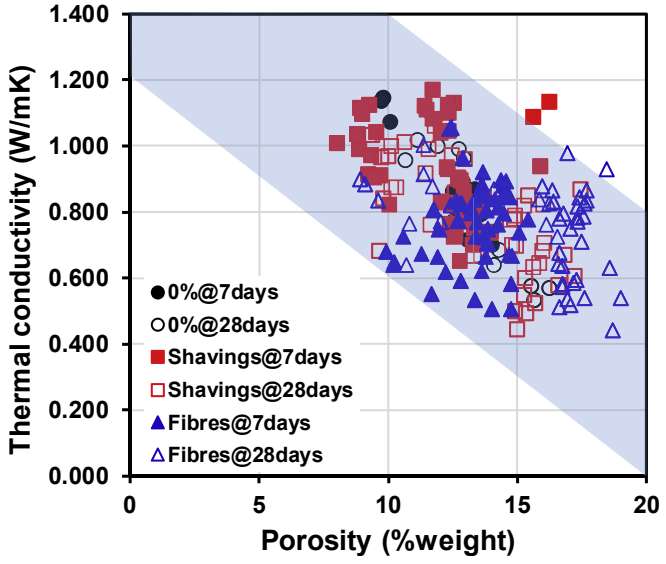

Fig. 16. Relationship between the thermal conductivity and porosity of the cement mortar specimens.

4. Conclusions

This paper has explained the influence of the type and amount of two different metallic waste materials on the volumetric, electrical, and thermal properties of cement-based mortars. The main conclusions in this article are summarised as follows:

- Based on the morphological analysis of the metallic waste, prior to the mixing process, steel wool fibres added to the mortars were shorter, much thinner and more homogeneous in shape and size than steel shavings.
- In addition, it was found that the mixing process tends to break the shavings reducing their length and enhancing their volumetric distribution on the mortar, making them less likely to form clusters than the steel wool fibres.
- Moreover, bulk density decreased with the addition of metallic waste, presenting higher reductions with shavings, due to their irregular shape, which is mainly attributed to an increase in the total volume of mortar. In contrast, porosity increased with the addition of metallic waste, especially in the case of fibres which enabled the formation of clusters due to their high ductility and slenderness.
- Additionally, it was proven that it is possible to evaluate the metallic waste distribution inside the mortars by ultrasonic tests. Mortars with both types of metallic waste presented a minimum ultrasonic time in the central zone of specimens,

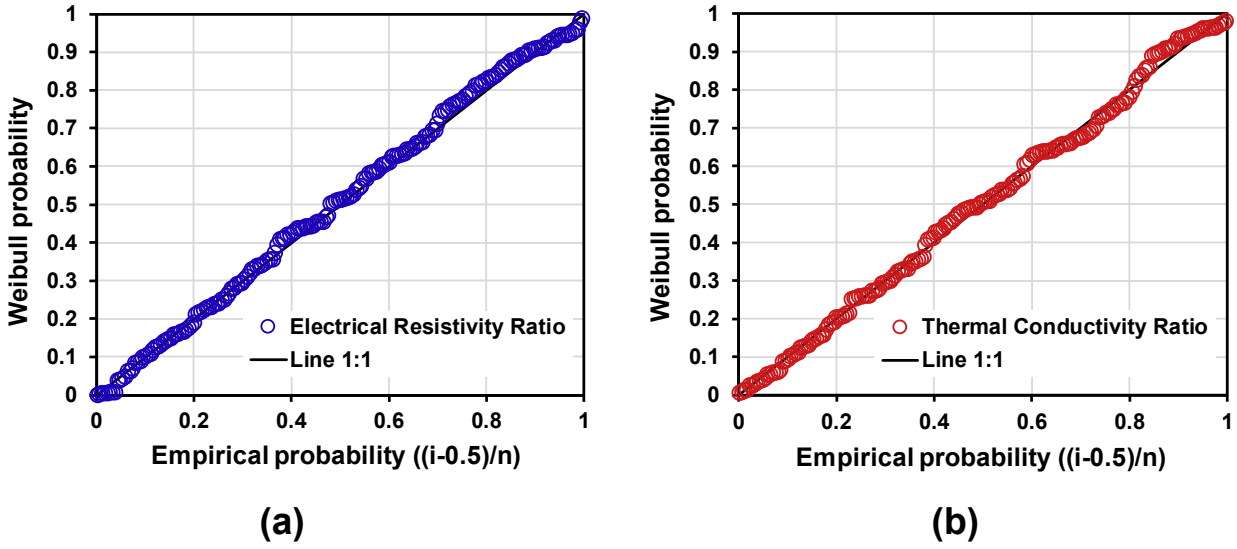

Fig. 17. Weibull probability-probability plots of the data ratios for (a) electrical resistivity and (b) thermal conductivity.

which is mainly attributed to the fibre migration process influenced by the mould boundary conditions during the vibration. Thus, ultrasonic pulse times were higher in the case of mortars with fibres. The scatter of the obtained results is related to the higher porosity found in these specimens.

- Furthermore, both types of metallic waste caused similar reductions in the electrical resistivity, but no percolation threshold was observed, which indicates that the fibre interconnection was not continuous along the material. Moreover, steel shavings caused an increase in the thermal conductivity of mortars, while the opposite tendency was observed for mortars containing steel fibres.
- Finally, based on a probabilistic analysis, it was concluded that both the type and amount of metallic waste, and the curing time used in this research did not present a significant influence on the variation of the electrical resistivity and thermal conductivity of the evaluated cement-based mortars.

Considering that the metallic waste addition did not compromise the electrical and thermal performance of the cement-based mortars, a second part of this study is currently being developed to evaluate the mechanical and crack self-monitoring properties of cement-based mortars by measuring the variation of their electrical resistance.

Acknowledgments

The authors would like to acknowledge the help provided by Poldie Oyarzun and Olga Iturra from the Laboratory Analysis of Solids (L.A.S-UNAB) and the Laboratory of Civil Engineering from the University Andres Bello. In addition, the authors would like to thank José L. Concha from LabMAT from University of Bio-Bio for the technical support given, and the company Sika S.A. Chile for the provision of the superplasticiser additive. Finally, Roque Borinaga wishes to thank the Basque Government for financial assistance through IT919-16 and the European Horizon 2020, since this work was partially funded by Joint Technology Initiative Shift2Rail through contract no.730841.

References

ASTM C128-01, 2001. Standard Test Method for Density, Relative Density (Specific Gravity), and Absorption of Fine Aggregate. ASTM International, West Conshohocken, PA.
ASTM C33-07, 2007. Standard Specification for Concrete Aggregates. ASTM International, West Conshohocken, PA.
ASTM C595/C595M-16, 2016. Standard Specification for Blended Hydraulic Cements. ASTM International, West Conshohocken, PA.
ASTM C642-13, 2013. Standard Test Method for Density, Absorption, and Voids in Hardened Concrete. ASTM International, West Conshohocken, PA.
ASTM D 5334, 2008. Standard Test Method for Determination of Thermal Conductivity of Soil and Soft Rock by Thermal Needle Probe Procedure. ASTM International, West Conshohocken, PA.
Banthia, N., Djeridane, S., Pigeon, M., 1992. Electrical resistivity of carbon and steel micro-fiber reinforced cements. Cement Concr. Res. 22 (5), 804–814.
Bentur, A., Mindess, S., 2007. Fiber Reinforced Cementitious Composites, second ed. Taylor & Francis, Abingdon, Oxon, UK.
Brandt, A.M., 2008. Fibre reinforced cement-based (FRC) composites after over 40 years of development in building and civil engineering. Compos. Struct. 86 (1), 3–9.
Cao, J., Chung, D.D.L., 2002. Damage evolution during freeze-thaw cycling of cement mortar, studied by electrical resistivity measurement. Cement Concr. Res. 32 (10), 1657–1661.
Çavdar, A., 2014. Investigation of freeze-thaw effects on mechanical properties of fiber reinforced cement mortars. Compos. B Eng. 58, 463–472.
Chung, D.D.L., 2012. Carbon materials for structural self-sensing, electromagnetic shielding and thermal interfacing. Carbon 50 (9), 3342–3353.
Corinaldesi, V., Mazzoli, A., Moriconi, G., 2011. Mechanical behaviour and thermal conductivity of mortars containing waste rubber particles. Mater. Des. 32 (3), 1646–1650.
EN 196-3:2005+A1:2009. Methods of testing cement-Part 3: Determination of setting times and soundness. CEN European Committee for Standardization, Brussels, Belgium.
García, A., Norambuena-Contreras, J., Partl, M.N., Schuetz, P., 2013. Uniformity and mechanical properties of dense asphalt concrete with steel wool fibers. Construct. Build. Mater. 43, 107–117.
Girardi, F., Giannuzzi, G.M., Mazzei, D., Salomoni, V., Majorana, C., Di Maggio, R., 2017. Recycled additions for improving the thermal conductivity of concrete in preparing energy storage systems. Construct. Build. Mater. 135, 565–579.
Khaliq, W., Kodur, V., 2011. Thermal and mechanical properties of fiber reinforced high performance self-consolidating concrete at elevated temperatures. Cement Concr. Res. 41 (11), 1112–1122.
Kim, D.J., Kang, S.H., Ahn, T.H., 2014. Mechanical Characterization of high-performance steel-fiber reinforced cement composites with self-healing effect. Materials 7 (1), 508–526.
Koenig, A., Dehn, F., 2016. Main considerations for the determination and evaluation of the acid resistance of cementitious materials. Mater. Struct. 49 (5), 1693–1703.
Lataste, J.F., Behloul, M., Breysse, D., 2008. Characterisation of fibres distribution in a steel fibre reinforced concrete with electrical resistivity measurements. NDT Int. 41 (8), 638–647.
Martinelli, E., Caggiano, A., Xargay, H., 2015. An experimental study on the post-cracking behaviour of hybrid industrial/recycled steel fibre-reinforced concrete. Construct. Build. Mater. 94, 290–298.
Meehan, D.G., Wang, S., Chung, D.D.L., 2010. Electrical-resistance-based sensing of impact damage in carbon fiber reinforced cement-based materials. J. Intell. Mater. Syst. Struct. 21 (1), 83–105.

Mindess, S., Young, J.F., Darwin, D., 2002. Concrete, second ed. Prentice Hall.
Nagy, B., Nehme, S.G., Szagri, D., 2015. Thermal properties and modeling of fiber reinforced concretes. Energy Procedia 78, 2742–2747.
Nguyen, D.L., Song, J., Manathamsombat, C., Kim, D.J., 2015. Comparative electro-mechanical damage-sensing behaviors of six strain-hardening steel fiber-reinforced cementitious composites under direct tension. Compos. B Eng. 69, 159–168.
Norambuena-Contreras, J., Castro-Fresno, D., Vega-Zamanillo, A., Celaya, M., Lombillo-Vozmediano, I., 2010. Dynamic modulus of asphalt mixture by ultrasonic direct test. NDT E Int. 43, 629–634.
Norambuena-Contreras, J., Gutierrez-Aguilar, V., Gonzalez-Torre, I., 2015. Physical and mechanical behaviour of a fibre-reinforced membrane with self-healing purposes via microwave heating. Construct. Build. Mater. 94, 45–56.
Norambuena-Contreras, J., Silva-Robles, E., Gonzalez-Torre, I., Saravia-Montero, Y., 2017. Experimental evaluation of mechanical and thermal properties of recycled rubber membranes reinforced with crushed polyethylene particles. J. Clean. Prod. 145, 85–97.
Norambuena-Contreras, J., Thomas, C., Borinaga-Treviño, R., Lombillo, I., 2016. Influence of recycled carbon powder waste addition on the physical and mechanical properties of cement pastes. Mater. Struct. 49 (12), 5147–5159.
Pacheco-Torgal, F., Jalali, S., 2011. Cementitious building materials reinforced with vegetable fibres: a review. Construct. Build. Mater. 25 (2), 575–581.
Quadir, U.M.T., Islam, K., Billah, A.M., Alam, M.S., 2016. Mechanical and durability properties of concrete using recycled granulated steel. Construct. Build. Mater. 123, 174–183.
Sengul, O., 2016. Mechanical behavior of concretes containing waste steel fibers recovered from scrap tires. Construct. Build. Mater. 122, 649–658.
Sevkat, E., Li, J., Liaw, B., Delale, F., 2008. A statistical model of electrical resistance of carbon fiber reinforced composites under tensile loading. Compos. Sci. Technol. 68 (10), 2214–2219.
Solgaard, A.O.S., Geiker, M., Edvardsen, C., Küter, A., 2014. Observations on the electrical resistivity of steel fibre reinforced concrete. Mater. Struct. Mater. Constr. 47 (1–2), 335–350.
Wang, Z., Dai, Q., Porter, D., You, Z., 2016. Investigation of microwave healing performance of electrically conductive carbon fiber modified asphalt mixture beams. Construct. Build. Mater. 126, 1012–1019.
Xie, P., Gu, P., Beaudoin, J.J., 1996. Electrical percolation phenomena in cement composites containing conductive fibres. J. Mater. Sci. 31 (15), 4093–4097.
Yoo, D.Y., Lee, J.H., Yoon, Y.S., 2013. Effect of fiber content on mechanical and fracture properties of ultra high performance fiber reinforced cementitious composites. Compos. Struct. 106, 742–753.
Zhutovsky, S., Hooton, R.D., 2017. Experimental study on physical sulfate salt attack. Mater. Struct. 50 (1), 54.